JEC JOURNAL OF ENERGY CHEMISTRY

Ceria on alumina support for catalytic pyrolysis of *Pavlova* sp. microalgae to high-quality bio-oils

Tevfik Aysu, Javier Fermoso and Aimaro Sanna

Citation: Journal of Energy Chemistry **27**, 874 (2018); doi: 10.1016/j.jechem.2017.06.014

View online: http://engine.scichina.com/doi/10.1016/j.jechem.2017.06.014

View Table of Contents: http://engine.scichina.com/publisher/scp/journal/JEC/27/3

Published by the Science China Press

Articles you may be interested in

Fractional pyrolysis of Cyanobacteria from water blooms over HZSM-5 for high quality bio-oil production
Journal of Energy Chemistry **23**, 732 (2014);

The effects of $K^{\pm}$ growth conditions on the accumulation of cesium by the bacterium *Thermus* sp. TibetanG6
Science in China Series C-Life Sciences **49**, 123 (2006);

Tingia unita sp. nov. (Noeggerathiales) with strobilus from the Lower Permian of Wuda, Inner Mongolia, China
Chinese Science Bulletin **51**, 2624 (2006);

The HetR-binding site that activates expression of *patA* in vegetative cells is required for normal heterocyst patterning in *Anabaena* sp. PCC 7120
Science Bulletin **60**, 192 (2015);

High-quality genomic study of a rubber plant
National Science Review **5**, 88 (2018);

Journal of Energy Chemistry 27 (2018) 874–882

Contents lists available at ScienceDirect

Journal of Energy Chemistry

journal homepage: www.elsevier.com/locate/jechem

http://www.journals.elsevier.com/journal-of-energy-chemistry/

Ceria on alumina support for catalytic pyrolysis of *Pavlova* sp. microalgae to high-quality bio-oils

Tevfik Aysu[a,b], Javier Fermoso[a], Aimaro Sanna[a,*]

[a] *Institute of Mechanical, Process and Energy Engineering (IMPEE), Heriot-Watt University, EH14 4AS Edinburgh, UK*
[b] *Department of Chemistry, Faculty of Education, Yuzuncu Yil University, 65080 Van, Turkey*

ARTICLE INFO

Article history:
Received 18 April 2017
Revised 23 June 2017
Accepted 29 June 2017
Available online 6 July 2017

Keywords:
Bio-oil
Pavlova sp.
Pyrolysis
Deoxygenation
Catalyst
Ceria

ABSTRACT

In this work, we report for the first time the in-situ catalytic pyrolysis of *Pavlova* sp. microalgae, which has been performed in a fixed-bed reactor in presence of Ce/Al_2O_3-based catalysts. The effects of pyrolysis parameters, such as temperature and catalyst were studied on the products yield distribution and bio-oil composition, among others. Results showed that all catalysts increased the bio-oil yield with respect to the non-catalytic runs and reduced the O/C ratio from 0.69 (*Pavlova* sp.) to 0.1–0.15, which is close to that of crude oil. In terms of bio-oil oxygen content, $MgCe/Al_2O_3$ presented the best performance with a reduction of more than 30%, from 14.1 to 9.8 wt%, of the oxygen concentration in comparison with thermal pyrolysis. However, $NiCe/Al_2O_3$ gave rise to the highest aliphatics/aromatics fractions. The elemental and gas analysis indicates that N was partially removed from the catalytic bio-oils in the gas phase in forms of NH_3 and HCN.

© 2017 Science Press and Dalian Institute of Chemical Physics, Chinese Academy of Sciences. Published by Elsevier B.V. and Science Press. All rights reserved.

1. Introduction

Microalgae have received much attention as a biofuel feedstock in response to the energy crisis, climate change and depletion of fossil fuels sources. The development of transportation fuels from microalgae would be economic feasible only if high-value co-products such as Omega-3 fatty acids (ω-3 FAs), plant sterols and protein-rich biomass are produced through the extraction of a fraction of microalgae to improve the economics of an integrated microalgae biorefinery [1]. *Pavlova* microalgae possess the potential to produce high amounts of ω-3 FAs such as eicosapentaenoic acid, EPA (C20:5) and docosahexaenoic acid, DHA (C22:6), which are used as dietary supplements and have been identified as a source of molecules with immunomodulation, antioxidant and antitumor activity [2,3]. In addition, *Pavlova* genera are among the most popular microalgae for the production of nutrients for fish, mollusc and shrimp in the aquaculture industry [4,5]. The extraction of these valuable micronutrients would leave behind a large mass of algae biomass as by-product, and pyrolysis might represent an interesting technology for its valorization producing liquid fuels and biogas. Pyrolysis is attracting particular interest among the technologies under development for the conversion of biomass feedstocks, due to its low capital and operational costs and the possibility to delocalize the densification of the biomasses where are produced. The densified bio-oils can then be refined in a centralized biorefinery and converted to final commercial fuels or chemicals.

Catalytic fast pyrolysis combines thermal decomposition with the catalytic transformation of pyrolysis vapours to less oxygenated liquid fuels by removing oxygen as CO, H_2O and CO_2, where the latter is most desirable since it would minimize the need for external H_2 [6–8]. Numerous are the catalysts reported in the literature for the catalytic fast pyrolysis of biomass; among which, acidic zeolites, and especially ZSM-5 [9–15], represent the most widely employed materials since their activity may be modulated by controlling the crystalline structure as well as the Si/Al ratios [8,14,16]. Nevertheless, other systems have been also evaluated which differ in either acidity or porosity, which are the most important properties influencing their catalytic activity [14,16,17]. The utilization of strong acid zeolitic catalysts achieves a high degree of bio-oil deoxygenation, which produces large concentrations of aromatic hydrocarbons. Nevertheless, high concentration of acid sites of the catalyst causes a sharp decrease in the bio-oil yield, because of excessive cracking. At the same time, the catalyst undergoes from extensive coking, which results in its fast deactivation [10,18–21].

Recently, a number of metal oxides including ZnO, MgO or CeO_2 were explored for lignocellulose catalytic pyrolysis [17,22,23]. Ceria-based catalysts have been shown effective in the conversion

* Corresponding author.
E-mail address: a.sanna@hw.ac.uk (A. Sanna).

http://dx.doi.org/10.1016/j.jechem.2017.06.014
2095-4956/© 2017 Science Press and Dalian Institute of Chemical Physics, Chinese Academy of Sciences. Published by Elsevier B.V. and Science Press. All rights reserved.

Downloaded to IP: 10.159.164.174 On: 2020-04-23 08:28:51 http://engine.scichina.com/doi/10.1016/j.jechem.2017.06.014

of oxygenates into ketonic-rich mono-functional molecules suitable for making hydrocarbon fuel components for gasoline, diesel, and jet fuel, with the highest carbon yield (23.5%) achieved on the pure CeO_2 [23]. Our research group has recently investigated the pyrolysis of different microalgae species, such as *Thalassiosira weissflogii* [24], *Tetraselmis* sp. [25], *Nannochloropsis* [26], *Isochrysis* sp. [25] and microalgae model compounds [24] in presence of Ceria and alumina based catalysts. It was shown that light organics, aromatics and aliphatics can be originated from carbohydrates, proteins and lipids, respectively. Also, CeO_2, $NiCe/Al_2O_3$ and $MgCe/Al_2O_3$ were able to decrease the oxygen content in the bio-oils and remove about a fifth of the starting N-content.

Although *Pavlova* sp. is a source of a number of high value-low volume products and could represent a good candidate for an integrated biorefinery, its evaluation as feedstock for biofuel production by catalytic pyrolysis has not been investigated so far. On the contrary, hydrothermal liquefaction has been employed to process Pavlova sp. at temperatures of 250, 300 and 350 °C, with and without Na_2CO_3. Maximum bio-oil yield was obtained at 350 °C (47.05 wt%) and the catalyst was linked to increase the conversion of carbohydrates [27].

Therefore, the objective of this work is to assess the potential of *Pavlova* sp. microalgae as feedstock for the production of biofuels by in-situ catalytic pyrolysis. Specifically, we selected Ce, MgCe and NiCe bimetallic species on alumina support, as they showed good catalytic activity with other microalgae [25,24]. This work studied their catalytic performance, pyrolysis products distribution, elemental analysis, chemical functionalities distribution (^{1}H NMR), chemical composition (GC–MS) and gas analysis (MS) at different temperatures. The extensive characterization of reactions products resulted in an improved understanding of *Pavlova* as biofuel feedstock.

2. Methodology

2.1. Raw material

The microalgae sample, *Pavlova* sp. was obtained from Varicon Aqua Solutions in liquid form (9 wt%) as raw biomass feedstock. The sample was dried in an oven at 60 °C for 8 h, ground and sieved to a particle size between 105 and 174 μm and stored in desiccator.

2.2. Catalysts preparation and characterization

Commercial ceria (CeO_2) nanopowder was purchased from Sigma-Aldrich. The synthetized ceria containing catalysts (Ce/Al_2O_3, $NiCe/Al_2O_3$ and $MgCe/Al_2O_3$) were prepared by means of the incipient wet impregnation method with $Ce(NO_3)_3\cdot 6H_2O$; $Mg(NO_3)_2\cdot 6H_2O$ and/or $Ni(NO_3)_2\cdot 6H_2O$ as precursors using alumina support (Sigma-Aldrich). The preparation method has been previously described elsewhere [24]. The Ce/Al_2O_3 catalyst preparation was carried out by stirring cerium (III) nitrate solution and alumina support at 300 rpm for 3 h at 80 °C. Then, the mixture was dried at 110 °C for 24 h. The dried $Ce(NO_3)_2/Al_2O_3$ was calcined in air at 600 °C for 3 h to obtain a theoretical 5 wt% Ce/Al_2O_3 and to achieve well dispersion [28]. The $NiCe/Al_2O_3$ catalyst was prepared by wet impregnating alumina with the cerium (III) nitrate solution and nickel (III) nitrate solution. The other catalysts were prepared using the same impregnation-calcination method described above.

N_2 physisorption isotherms at −196 °C were measured on a Micromeritics Gemini VII instrument. The catalyst samples were degassed overnight at 180 °C. The surface areas were determined using the Brunauer–Emmett–Teller (BET) equation, and the pore size distributions were calculated by applying Barrett–Joyner–Halenda (BJH) method. The crystalline phases of the catalysts were identified by powder X-ray diffraction using Bruker D8 Advance powder diffractometer, operating with Ge-monochromated Cu $K\alpha 1$ radiation (wavelength = 1.5406 Å, 40 kV, 30 mA) and a Lynx-Eye linear detector in reflectance mode. Data were collected over the angular range 5°–85° degrees in 2θ under atmospheric pressure.

Lewis and Brønsted acid sites in $NiCe/Al_2O_3$ were determined by performing FTIR of pyridine adsorbed samples (at 150 °C) using a Harrick made Praying Mantis cell attached to a PerkinElmer Spectrum GX instrument. The samples were previously desorbed in situ at 150 °C under a nitrogen flow and then, pyridine was injected into the sample for 60 min at room temperature. Excess pyridine was flushed by flowing nitrogen at 150 °C before recording the spectra.

2.3. Feedstocks and products analyses

2.3.1. Proximate and ultimate analysis

The moisture content and the proximate analyses in dry basis (volatile matter (VM) and ash content (A)) of the dried *Pavlova* sp. and biochars were conducted according to ASTM standards: D2016, E872-82, D1102-84, respectively. Then, the fixed carbon, FC, was determined by difference according to the equation: FC = 100 – VM – A. Therefore, the term (FC) refers to the organic solid matter (i.e., without ash) that remains after the total volatiles of a solid fuel are thermally released under inert atmosphere. In addition, the ultimate analysis of the raw material and reaction products (biochar and bio-oil) was carried out in a LECO CHNS-932 analyser to determine the content of C, H, N and O (by difference).

2.3.2. Proton nuclear magnetic resonance (^{1}H NMR) analysis

^{1}H NMR analyses of the *Pavlova* sp. pyrolysis bio-oils were performed using a Bruker Avance III operating at 400 MHz. the samples were dissolved in $CDCl_3$ (1:1 volume ratio) and TMS (tetramethylsilane) was used as internal standard.

2.3.3. Thermogravimetric analysis

Thermogravimetric analysis was carried out using a TA Q500 thermogravimetric analyser. TG-pyrolysis using N_2 as carrier gas was used to determine the moisture content, volatile matter and fixed carbon and to compare/confirm with the results obtained by ASTM standards. TG-combustion using air as carrier gas was used to determine the ash content. The samples, weighing approximately 10 mg, were heated from 25 to 800 °C at a constant heating rate of 20 °C/min under N_2 atmosphere and then the temperature was decreased to 600 °C to determine the fixed carbon and ash contents under air atmosphere. The loss of weight between 25 and 105 °C was used to calculate the sample moisture content. The volatile matter content of the raw material was determined from the weight loss between 105 and 600 °C as primary volatiles, and 600 and 800 °C as secondary volatiles. The ash content of the sample was determined from the amount of solids that remains at the end of the combustion step. Fixed carbon was calculated by subtracting the ash content from the solids remaining at the end of run.

2.3.4. GC–MS and gas analysis

Agilent GC–MS 7890A/5975C series (Agilent Technologies, Santa Clara, CA) was used for the semi-quantitative GC–MS analysis of produced bio-oils. The column was an HP 235-INNOWAX with 60 m length, 0.250 mm inner diameter, 0.25 µm film having temperature limits between 40 °C to 300 °C. GC and the injector temperatures were the same during analysis. Helium was used as the carrier gas at a flow rate of 1.7 mL/min. 1 μL samples was injected with a split ratio of 1:20. The GC oven temperature program was as follows: start at 40 °C; hold for 10 min, raise from 40 °C to 200 °C

Downloaded to IP: 10.159.164.174 On: 2020-04-23 08:28:51 http://engine.scichina.com/doi/10.1016/j.jechem.2017.06.014

at a heating rate of 5 °C/min; hold for 15 min, raise to 240 °C at a heating rate of 10 °C/min; hold for 15 min, raise to 260 °C at a heating rate of 10 °C/min; hold at the final temperature for 10 min. The end of column was directly introduced into the ion source of a mass selective detector of Agilent 5975C series with operating conditions of transfer line at 270 °C, ion source at 250 °C and electron energy of 70 eV. Identification of bio-oil components was done using mass spectral libraries (PMW_Tox3.l, Wiley7n.1 and NIST05a.L). During pyrolysis of *Pavlova* sp., the permanent gases were collected in a gas bag and analyses by a MKS Cirrus II Mass Spectrometer.

2.4. Pyrolysis experiments

The pyrolysis experiments of *Pavlova* sp. were performed using a fixed-bed reactor described elsewhere [26]. The biomass sample was dried at 105 °C overnight before pyrolysis runs. In a typical run, 3 g of dried *Pavlova* sp. powder or a mixture of dried *Pavlova* sp. and catalyst (1:1) was placed into the reactor in a ceramic boat shape crucible. Then, the reactor was closed tightly and N_2 gas was fed at a flow rate of 15 mL/min for 10 min to remove the air in the reactor before pyrolysis. The reactor is heated by an external electric furnace, whose temperature was regulated by a temperature controller and the sample temperature measured by a K type thermocouple. The catalytic and non-catalytic pyrolysis experiments of *Pavlova* sp microalgae were performed at a heating rate of 100 °C/min up to three different maximum temperatures of 450, 500 and 550 °C, and held for 60 min. The volatiles so generated in the pyrolysis zone were swept by a N_2 flow of 15 mL/min to leave rapidly the reaction zone, being condensed by the bio-oil condensation system, which consisted of 3 Dreschel bottles maintained at ≈ 0 °C on an ice-water bath. Permanent gaseous products were not collected and vented out together with the N_2. The condensed bio-oils were recovered using acetone. The reactor was also washed with 100 mL of acetone to account for oil condensed between the heated region and the condensation system. The biochar was fully recovered from the reactor, so vestiges of it into the condensation system were not observed in any of the runs. Then the solvent was evaporated at 40 °C and 11 kPa using a rotary evaporator to recover the oil which was recorded as bio-oil yield. When the reactor was cooled to room temperature, the remaining solid left behind was taken out, weighed and recorded as biochar yield (subtracting the catalyst weight). The mass yield of i pyrolysis products (i = *bio-oil* and *biochar*) was determined following Eq. (1). Then, gas yield was calculated by subtraction of these products from the microalgae fed.

$$\text{Mass yield}_i\ (\text{wt\%}) = \frac{W_i}{W_{\text{microalgae,db}}} \cdot 100 \quad (i = \text{bio} - \text{oil and biochar}) \tag{1}$$

where $W_{\text{microalgae,db}}$ and $W_{\text{biochar,db}}$ are the weights (on dry basis) of initial microalgae and the remaining solid (biochar), respectively.

The elemental (C, H and O) mass balances were also assessed from the yield of the different products and their ultimate analyses. Thus, the nitrogen distribution, N_i, between the different i fractions was calculated according to Eq. (2):

$$N_i(\text{wt\%}) = \frac{N_i}{N_{\text{Pavlova}}} \cdot 100 \ (i = \text{bio} - \text{oil and biochar}) \tag{2}$$

where N_{Pavlova} is the and nitrogen content in the *Pavlova* sp.

The high heating value (HHV) of the microalgae and of the different fractions was calculated according to Eq. (3), which is a correlation reported to be valid for solid and liquid fuels [29]:

$$\text{HHV (MJ/kg}_i) = 0.3491 \cdot C + 1.1783 \cdot H + 0.1005 \cdot S - 0.1034 \cdot O - 0.0151 \cdot N - 0.0211 \cdot A \tag{3}$$

Table 1. Main characteristics of *Pavlova* sp. microalgae.

Components	
Moisture (%)	10.14
Proximate analysis[a] (wt%)	
Ash	27.21
Volatile matter	59.93
Fixed carbon	12.86
Ultimate analysis[a] (wt%)	
Carbon	33.90
Hydrogen	4.22
Nitrogen	3.50
Oxygen[b]	31.17
H/C molar ratio	1.50
O/C molar ratio	0.69
Higher heating value (MJ/kg)	12.96
Chemical composition (wt%)	
Protein	43
Lipid	20
Carbohydrate	26

[a] Dry basis.
[b] By difference.

where *C, H, O, N, S* and *A* represent carbon, hydrogen, oxygen, nitrogen, sulphur and ash contents of i, expressed in wt% on dry basis.

Then, the energy yield of any i fraction was calculated according to Eq. (4), whilst the gas energy yield was determined by difference.

$$\text{Energy yield}_i(\%) = \frac{\text{Mass yield}_i \cdot \text{HHV}_i}{\text{HHV}_{\text{Pavlova}}} \cdot 100 \quad (i = \text{bio} - \text{oil and biochar}) \tag{4}$$

3. Results and discussion

3.1. Pavlova *sp. characterization*

Before the pyrolysis experiments, *Pavlova* sp. was characterized by means of the determination of the proximate and ultimate analyses, as well as the chemical composition (see Table 1) to evaluate the potential for production of bio-oil. The *Pavlova* sp. contains relatively low lipid amount (20 wt%) that makes this algae not ideal for biodiesel production; but potentially suitable for pyrolysis, due to its protein content (43 wt%), which is in good agreement with literature (40.5–65 wt%) and consistent with other algal species studied for production of biofuels [30–33]. In addition, *Pavlova* carbohydrates content (26%) is relatively larger than microalgae average [34]. Concerning proximate analysis (expressed in dry basis), this microalgae contains fairly low volatile matter (59.9 wt%), whilst accounts for relatively high ash content (27.2 wt%) and similar fixed carbon (12.9 wt%) in comparison with other algal species (such as *Chlorella, Scenedesmus almeriensis* and *Nannochloropsis gaditana*, among others), which contain 62–80, 7–19, and 10–18 wt%, respectively [25,32,35]. Regarding to its elemental analysis (expressed in dry basis), it contains C, H, N and O in 33.9, 4.2,3.5 and 31.2 wt%, respectively; which are significantly lower in terms of C, H and N in comparison with other types of microalgae that accounts with values of 39–49, 6–8, 6–9 wt%, respectively [31,32,35,36]. The low C and H contents and the large ash content result in the microalgae having low higher heating value (12.96 MJ/kg).

Fig. 1 shows the TG derivative weight loss profile (in wt%/min) for the *Pavlova* sp. microalgae during its pyrolysis in N_2 atmosphere up to 800 °C. As a whole, this curve can be divided into three stages: loss of moisture, devolatilization, and decomposition of the carbonaceous matter. The loss of moisture takes place as a consequence of the sample physically re-adsorbed water after the

Downloaded to IP: 10.159.164.174 On: 2020-04-23 08:28:51 http://engine.scichina.com/doi/10.1016/j.jechem.2017.06.014

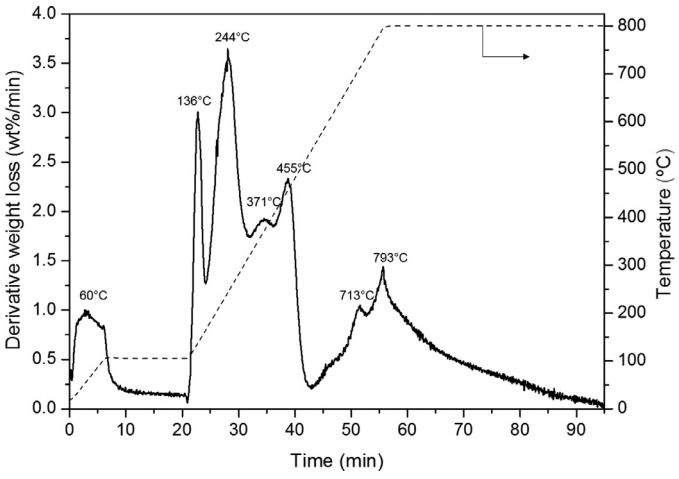


Fig. 1. Derivative weight loss profile of *Pavlova* sp. microalgae. (Reaction conditions: 100 mL/min N_2; heating rate, 15 °C/min from room temperature to 800 °C.)

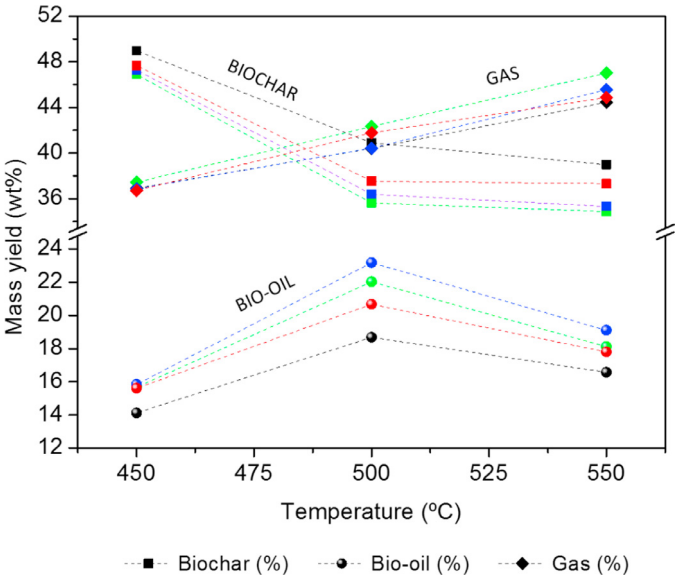


Fig. 2. Products yield distribution obtained in the catalytic and non-catalytic pyrolysis tests of *Pavlova* sp. as a function of reaction temperature. Non-catalytic: black; Ce/Al_2O_3: green; $NiCe/Al_2O_3$: blue; $MgCe/Al_2O_3$: red. (For interpretation of the references to colour in this figure legend, the reader is referred to the web version of this article.)

drying process. This step happened at $T < 105$ °C, with a maximum rate at around 60 °C. Then, the main devolatilization stage occurred at temperatures between 120 and 500 °C, which comprises four well defined peaks (with maximum decomposition temperatures at 136, 244, 371 and 455 °C) that involves microalgae compounds devolatilization (carbohydrates, proteins and lipids). The first event at 136 °C might be due to evaporation of water trapped between the thick microalgae cells walls. Thus, according to previous studies the devolatilization of proteins, cellulose, and lipids was reported to happen at 220–300, 375 and 460 °C, respectively [24]. Finally, the last decomposition step takes place at $T > 550$ °C, corresponds to the secondary decomposition of char formed in the previous steps. The latter event may also involve further proteins decomposition.

3.2. Catalysts characterization

The total pore volume, specific surface area (S_{BET}) and average pore diameter of Al_2O_3 support were 0.129 cm^3/g, 75.39 m^2/g, and 37.44 Å, respectively. The incorporation of a metal oxide to the Al_2O_3 support modified the catalyst properties. Thus, whereas surface area and pore volume were reduced, the average pore size barely varied. Surface areas of Ce/Al_2O_3, $NiCe/Al_2O_3$, and $MgCe/Al_2O_3$ were found to be 55.12, 60.25, and 49.58 m^2/g, respectively [26]. The X-ray diffraction patterns of the prepared catalysts with Al_2O_3 support are shown in the Supplementary content (Fig. S1). The diffraction patterns confirm the formation of CeO_2, NiO, MgO metal oxides with exact matches in the catalysts prepared with Al_2O_3 support. XRD patterns of Ce/Al_2O_3 catalyst exhibit peaks at 2θ scale = 28.5°, 33.10°, 47.60°, 56.39°, 59.13°, 69.51° and 79.10° attributed to the cubic cerium (IV) oxide crystal phase. XRD patterns of $Ni–Ce/Al_2O_3$ show peaks that match the cubic nickel (II) oxide at $2\theta = 37.20°$, 43.18°, 62.90°, 75.22° and 79.40°. $MgCe/Al_2O_3$ catalyst shows peaks for cubic magnesium oxide (MgO) crystal at 2θ scale = 37.00°, 43.00°, 62.30°, and 78.50°. These results were consistent with those previously reported in literature [37,38].

Fig. S2 shows the infrared spectra of pyridine adsorbed on the $NiCe/Al_2O_3$ catalyst surface. The bands corresponding to the Lewis (L) acid sites (~1450 cm^{-1}) and Brønsted (B) acid sites (1640 cm^{-1}) were detected. The typical Brønsted acid sites band at 1540 cm^{-1} was not detected, but could have been possibly shifted to the peak found at 1530 cm^{-1}. Also, a band located at ~1596 cm^{-1} (H) correspond to hydrogen-bonds between pyridine and the surface of the catalyst was denoted [39].

3.3. Catalytic pyrolysis of Pavlova sp.

Temperature is an important factor affecting the performance of microalgae pyrolysis, concerning the products yield distribution and their composition [40]. Biomass depolymerization occurs when temperature is increased over activation energies necessary to break bonds, resulting in the formation of free radicals and fragmented species that originates bio-oil components and non-condensable gases. Fig. 2 displays the distribution of the products obtained by catalytic and non-catalytic pyrolysis of *Pavlova* sp. at temperatures between 450 and 550 °C. In this figure is appreciated that whereas the gas fraction continuously rose with reaction temperature, the bio-oil production experienced a maximum at 500 °C. This behavior of maximum production of bio-oil at 500 °C has been also observed by other authors in the literature [36,41]. Nevertheless, the biochar production sharply decreases up to 500 °C, keeping almost unaltered at higher temperatures. The high ash content of this microalgae specie (see Table 1) together with some experimental conditions, such as the low heating rate (100 °C/min) and the relatively high residence time (about 9–12 s) significantly affected the products distribution and is probably responsible for the high biochar yields (35–49 wt%) [34,40].

Fig. 2 also shows how all the ceria-based catalyst employed in the present work increased the microalgae conversion (mostly from 450 to 500 °C) in terms of bio-oil and gas production, in comparison with the non-catalytic performance and exhibited similar effects on the product yields distribution, being more noticeable at 500 °C. All the catalysts increased the bio-oil production with respect to the non-catalytic performance, mostly at expenses of the biochar fraction. In this respect, $NiCe/Al_2O_3$ followed by Ce/Al_2O_3 was the most effective catalysts in terms of bio-oil production with 23.2 and 22.0 wt% at 500 °C. The biochar yield decreased slightly more in presence Ce/Al_2O_3 than other catalysts; which has been already observed in the pyrolysis of different algal strains with similar composition (high protein and low lipid) [26].

As a result of best pyrolysis performance occurred at 500 °C in terms of bio-oil yield, bio-oils and biochars produced at this

Downloaded to IP: 10.159.164.174 On: 2020-04-23 08:28:51 http://engine.scichina.com/doi/10.1016/j.jechem.2017.06.014

Table 2. Elemental analysis of biochars and bio-oils obtained with different ceria based catalysts at 500 °C from *Pavlova* sp.

Pyrolysis product	Elemental analysis (wt%)[a]	No catalyst	Ce/Al_2O_3	$NiCe/Al_2O_3$	$MgCe/Al_2O_3$
Biochar	C	19.48	19.07	19.38	18.72
	H	0.47	0.49	0.47	0.50
	N	1.55	1.54	1.53	1.55
	O[b]	18.01	18.33	18.03	18.50
	Ash	60.49	60.57	60.59	60.73
	HHV (MJ/kg)	4.19	4.04	4.16	3.91
Bio-oil	C	68.31	74.19	71.70	74.80
	H	8.84	9.22	8.86	9.14
	N	8.75	6.32	6.62	6.27
	O[b]	14.10	10.27	12.82	9.79
	HHV (MJ/kg)	32.67	35.61	34.04	35.78

[a] Dry basis.
[b] By difference.

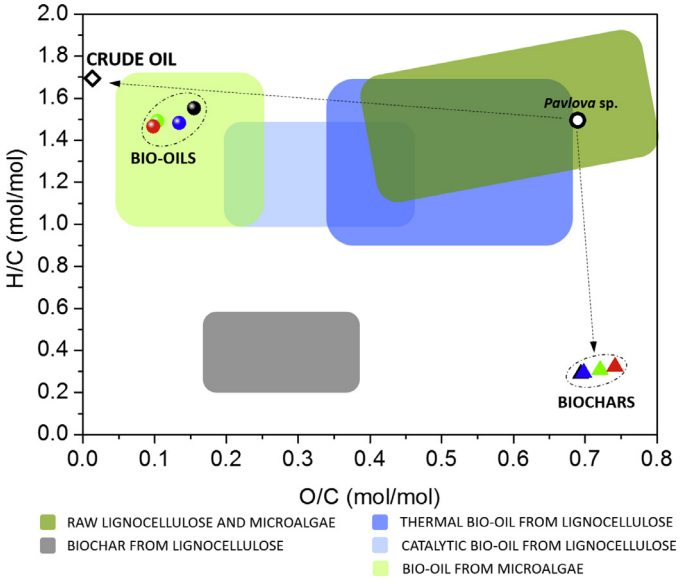


Fig. 3. van Krevelen diagram of *Pavlova* sp. and its pyrolysis products: biochar (Δ) and bio-oil (○). Non-catalytic: black; Ce/Al_2O_3: green; $NiCe/Al_2O_3$: blue; $MgCe/Al_2O_3$: red [8,23,29]. (For interpretation of the references to colour in this figure legend, the reader is referred to the web version of this article.)

temperature were selected for further analysis and evaluation of the catalysts activity.

The elemental analysis (dry basis), ash content and HHV of biochars generated from *Pavlova* sp. at 500 °C using different ceria-based catalysts are reported in Table 2. From this table can be stated that the elemental composition of all biochars is rather similar, revealing that it does not depend on the catalyst employed. In addition, *Pavlova* sp. loses C and O in a rather similar proportion during pyrolysis. Thus, Fig. 3 shows the H/C vs O/C molar ratios by means of a van Krevelen diagram for biochars and bio-oils originated from *Pavlova* sp. pyrolysis in comparison with those derived from lignocellulose and raw feedstocks [8,36,40]. In this figure can be observed that biochars derived from *Pavlova* sp. contain much less C and are richer in O than typical biochars from lignocelluloses, which normally are enriched in carbon while lose a great fraction of the oxygen originally contained in the raw biomass [8].

The carbon to nitrogen ratio (C/N) demonstrates the ability for an organic substrate to release inorganic nitrogen when mixed with soil [42]. Biochars usually present C/N ratios that vary between 7 and 500 depending on the precursor and pyrolysis conditions. Thus, a C/N ratio of ≈ 14, together with the large ash content, make these *Pavlova* sp. derived biochars as good candidate for soil amendment rather than for fuel only 3.9-4.2 $MJ/kg_{biochar}$).

The composition of the non-condensable gases released during the pyrolysis experiments was detected as summarized in Fig. 4. CO_2, H_2O and CO were the predominant compounds. All the catalysts increased the decarbonylation reactions, while CO_2 elimination was the main oxygen removal pathway. Permanent gases are formed in primary biomass decomposition and secondary cracking and related reforming reactions, where CO_2 formation is mainly due to primary pyrolysis, while formation of CO is mostly during the secondary pyrolysis stage [43]. Around 14–15 vol% of light hydrocarbons were observed in the gaseous product obtained with the catalysts, being MgCe the most effective. These values are close to those obtained by *Chlorella* pyrolysis in presence of ZSM-5 [44]. On the contrary, only about 4% of C_1–C_5 hydrocarbons were produced in absence of catalysts, suggesting that MgCe, NiCe and Ce on alumina promote cracking reactions. Moreover, an indication of the cracking capacity of protein macromolecules is given by the increased volume of NH_3 and HCN in the gases produced with the ceria-based catalysts. In a previous work, we already shown that Ce is able to increase the cracking of protein model compounds generating similar amounts of HCN (8 vol%) and NH_3 (2%) [24].

The composition and properties of the bio-oils obtained by microalgae pyrolysis are generally very different compared to those of conventional bio-oils derived from lignocellulosic biomass, due to differences in their composition [40].

The elemental analysis of bio-oils generated from *Pavlova* sp. at 500 °C using different ceria-based catalysts is also summarized in Table 2, where an enrichment of between 5 and 10 wt% in C, and up to 4 wt% in H can be observed for those bio-oils generated in presence of a ceria-based catalyst, in comparison with that obtained without catalyst. Moreover, these bio-oils contained significantly less oxygen (≈14 wt% in non-catalytic, and 10–13 wt% for catalytic bio-oils) than those bio-oils typically obtained from lignocellulosic biomass (30–45 wt% in non-catalytic, and 20–40 w% in catalytic bio-oils) [8]. Thus, this behaviour is reflected in the van Krevelen diagram shown in Fig. 3, where the pyrolysis bio-oils values are shifted to lower O/C ratios (0.1–0.15) than the original microalgae (0.69), getting closer to the crude oil. Then, the use of ceria-based catalysts gave rise to an improvement in the HHV of these bio-oils in comparison with non-catalytic one, which rises from 32.7 to 34 – 35.8 $MJ/kg_{bio-oil}$, respectively. In particular, the utilization of CeO_2/Al_2O_3 and $NiCe/Al_2O_3$ produced a bio-oil that preserve ≈ 61% of the energy initially contained in the *Pavlova* sp. in comparison with hardly ≈47% in case of the non-catalytic pyrolysis to the detriment of biochar and gas fractions.

High nitrogen content of non-catalytic bio-oil (8.8 wt%), which derives from chlorophyll and proteins in *Pavlova* sp. was somehow reduced when the catalysts were used (6.3–6.6 wt%) and

Downloaded to IP: 10.159.164.174 On: 2020-04-23 08:28:51 http://engine.scichina.com/doi/10.1016/j.jechem.2017.06.014

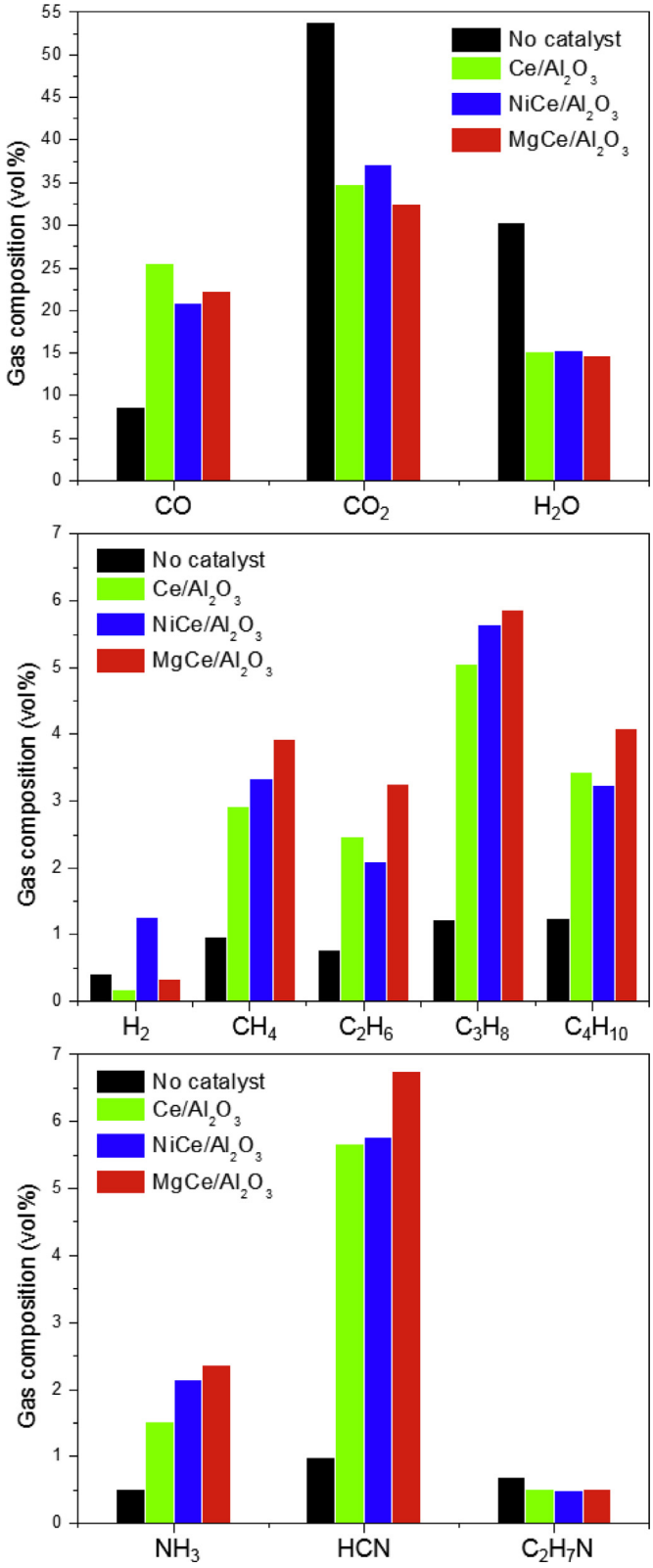


Fig. 4. Gas composition (by mass spectrometer, MS) obtained during catalytic and non-catalytic *Pavlova* sp. pyrolysis between 400 and 500 °C.

preferentially sent to gas phase as shown in Fig. S3, in which is displayed the N distribution among the pyrolysis products.

However, whereas there are not noteworthy differences in the elemental analysis of bio-oils obtained from *Pavlova* sp. with the ceria-based catalysts used in this study, their overall chemical composition clearly differs. Thus, Table 3 summarizes the integration of the ^{1}H NMR spectra of these bio-oils, which is of great importance, since it gives a complete overview of the chemical functionalities present in the bio-oils. The region of the spectra, from 0 to 1.5 ppm, representing aliphatic protons was the more populated for all bio-oils (>40% of all protons) indicating their high aliphatic content. However, all the catalysts showed an increased in the aliphatic content from 15% ($MgCe/Al_2O_3$) up to 39% ($NiCe/Al_2O_3$). *Pavlova* had a less pronounced production of alkanes compared to *Nannochloropsis*, which resulted in 62% protons in the region 0–1.5 ppm using $NiCe/Al_2O_3$ [26]. The next integrated region (1.5–3.0 ppm) represents protons on aliphatic carbon atoms that may be bonded to a C=C double bond (aromatic or olefinic) or are two bonds away from a heteroatom. All bio-oils contain high levels of protons in this spectral region. The next portion of the spectrum, 3.0–4.4 ppm, might represent protons on carbon atoms next to an aliphatic alcohol or ether, or a methylene group that joins two aromatic rings. The appearance of these oxygenated compounds (11.6% in non-catalytic bio-oil), experienced a significant reduction (>46%) as a consequence of the catalyst, especially in case of Ni containing ceria-based catalyst (70% of reduction). The region between 4.4 and 6.0 ppm represents aromatic ether protons and many of the hydrogen atoms of carbohydrate-like molecules. These types of molecules are in small amount in all the bio-oils, from ≈5% (non-catalytic) up to ≈0.6% ($NiCe/Al_2O_3$). This is consistent with the low O content of these bio-oils, especially for those obtained by using Ce/Al_2O_3 and $NiCe/Al_2O_3$ as discussed above. The aromatic region of the spectrum (6.0 to 9.5 ppm) contains from 9.5% (non-catalytic) up to just 12.3% ($MgCe/Al_2O_3$) of the protons in the bio-oils. This represents not only those hydrogen atoms in benzenoids, but also those in hetero-aromatics containing O and N. Then, aldehydes and carboxylic acids, which appear in the downfield spectral regions (9.5 to 10 ppm) were not detected in any of the bio-oils. This is a representative difference in comparison with lignocellulosic derived bio-oils, which are particularly rich in the latter compounds, such as acetic acid and hydroxyacetaldehyde. Overall, the ^{1}H NMR analysis shows that aliphatic protons are most prevalent for those bio-oils derived from *Pavlova* sp. as has been previously reported for other microalgae [25,26]. However, whereas all the catalysts increased the aliphatic compounds, they decreased the total oxygenated in comparison with non-catalytic bio-oil.

Then, the individual chemical compounds contained in the bio-oils from the microalgae pyrolysis at 500 °C were identified by GC–MS as shown in Fig. 5. It was estimated that about 44% of the bio-oil compounds could be detected by GC–MS. The compounds were grouped for functionalities to better understand the effect of the catalysts (Table S1 shows the complete list of identified compounds in bio-oils).

Kumar et al. [45] have recently reviewed the thermochemical and catalytic conversion of microalgae. According to this review, Fig. 6 shows a simplified schematic diagram of the proposed reaction mechanisms experienced by the three main components (i.e. proteins, lipids and carbohydrates) to produce aromatic and polyaromatic compounds. Proteins undergo a series of cracking reactions that involves their conversion to final aromatics (such as toluene and styrene), which then can polymerized to polycyclic aromatic hydrocarbons (PAH). During these processes, deamination reactions occur, and are reflected in a higher concentration of NH_3 and HCN species in the gas phase as shows Fig. 4. The main monoaromatics (MA) formed were phenol and phenol and benzene substitutes. $NiCe/Al_2O_3$ produced the largest fraction of MA (~20% of which 5.6% benzenes).

Carbohydrates suffer cracking to smaller organic moieties like alcohols, acids, aldehydes, and ketones; which undergo deoxygenation (decarboxylation, decarbonylation and dehydration) and are then cracked into olefins; to finally experience a series of aromatization reactions to yield different aromatics.

Downloaded to IP: 10.159.164.174 On: 2020-04-23 08:28:51 http://engine.scichina.com/doi/10.1016/j.jechem.2017.06.014

Table 3. ^{1}H NMR Integrations of *Pavlova* sp. bio-oils formed with ceria based catalysts at 500 °C versus specific chemical shift ranges.

Chemical shift region (ppm)	Proton assignment	Hydrogen content (% of all hydrogen)			
		No catalyst	Ce/Al_2O_3	$MgCe/Al_2O_3$	$NiCe/Al_2O_3$
0.0–1.5	Alkanes	40.476	50.078	46.471	56.180
1.5–3.0	Aliphatics α-to heteroatom or unsaturation	33.324	32.508	32.743	29.741
3.0–4.4	Alcohols, ether, methylene-dibenzene	11.672	6.262	5.337	3.467
4.4–6.0	Methoxy, methoxybenzene, carbohydrates	4.990	1.169	3.090	0.629
6.0–9.5	(Hetero-) aromatics	9.552	10.205	12.342	10.099
9.5–10.0	Aldehydes	–	–	0.017	–

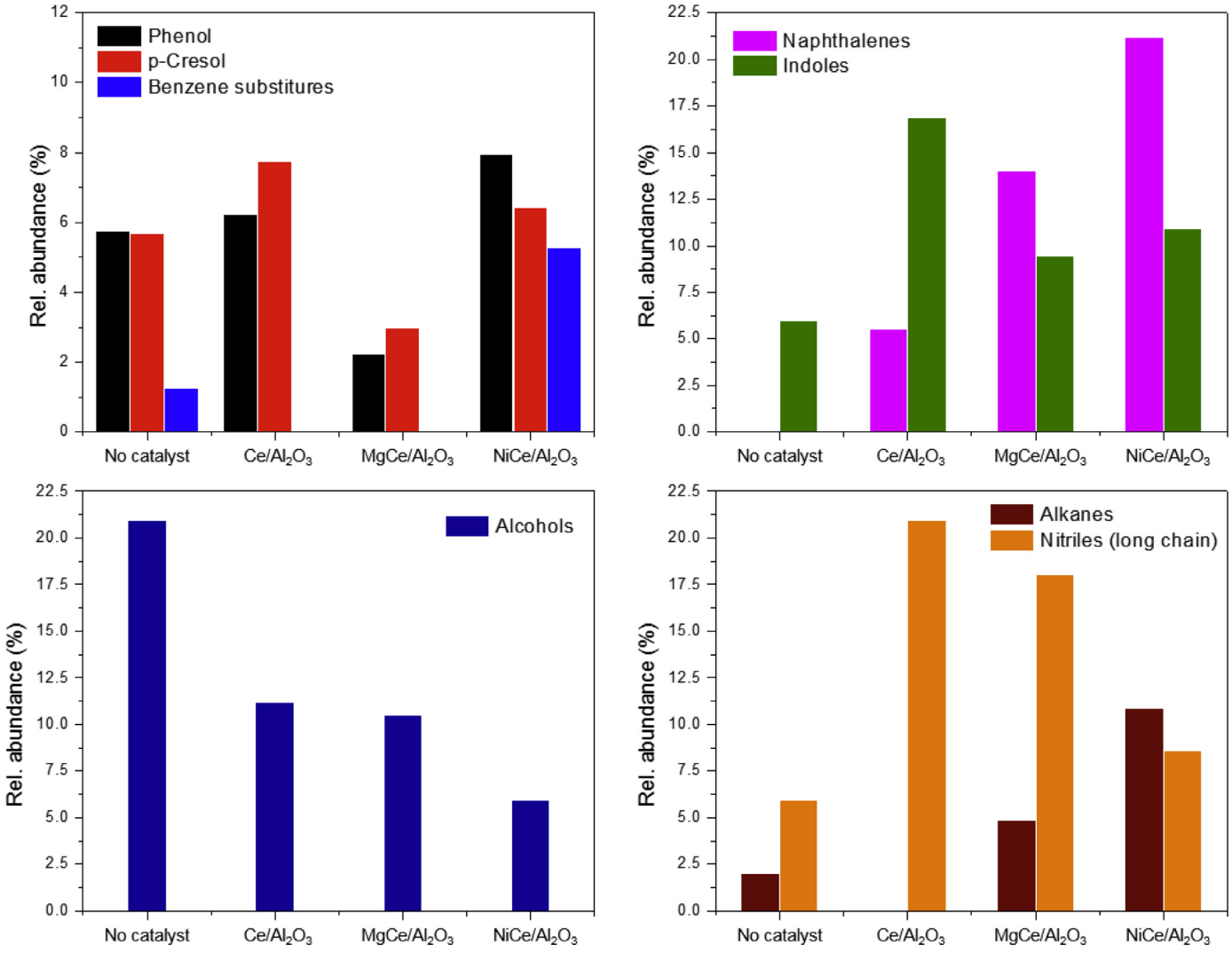


Fig. 5. Catalytic and non-catalytic bio-oil compounds grouped in chemical functionalities from GC–MS analysis.

The third components of microalgae (lipids) are thermally decomposed to heavy hydrocarbons by decarboxylation, dehydration and decarbonylation, and these in turn are cracked into olefins, which are accordingly converted into aromatics.

The presence of all the catalysts led to formation of N-heterocyclic compounds such as indoles and PAH (mainly naphthalenes). Even in this case, $NiCe/Al_2O_3$ resulted in the highest PAH relative yield suggesting increased aromatization and polymerization effect. The formation of aromatic and PAH was explained by secondary reactions during pyrolysis, based on Diels–Alder and deoxygenation of oxygenated aromatic compounds mechanisms [46]. Although, MA was formed, the combined information from ^{1}H NMR and GC–MS indicates that these metal oxides catalysts do not significantly enhance the formation of aromatics compared to zeolites, such as HZSM-5 [47]. Instead, indoles formation was favoured by $Ce\text{-}Al_2O_3$. Alcohols were represented mainly by phytol ($C_{20}H_{40}O$), an acyclic diterpene alcohol, whose formation decreased in presence of the three catalysts in the following order: Ce > MgCe > NiCe, indicated that NiCe was the most active in cracking down these large molecules. This trend is confirmed by the abundance of the bio-oils protons in the chemical shift region 3–4.4 ppm (see Table 3). Finally, long chain nitriles (e.g. hexadecanenitrile and tetradecanenitrile) were abundant in presence of Ce and MgCe, while decreased of about 50% in presence of NiCe. In the same time, long chain aliphatic hydrocarbons such as tridecane, pentadecane and tetradecane were detected when NiCe was

Downloaded to IP: 10.159.164.174 On: 2020-04-23 08:28:51 http://engine.scichina.com/doi/10.1016/j.jechem.2017.06.014

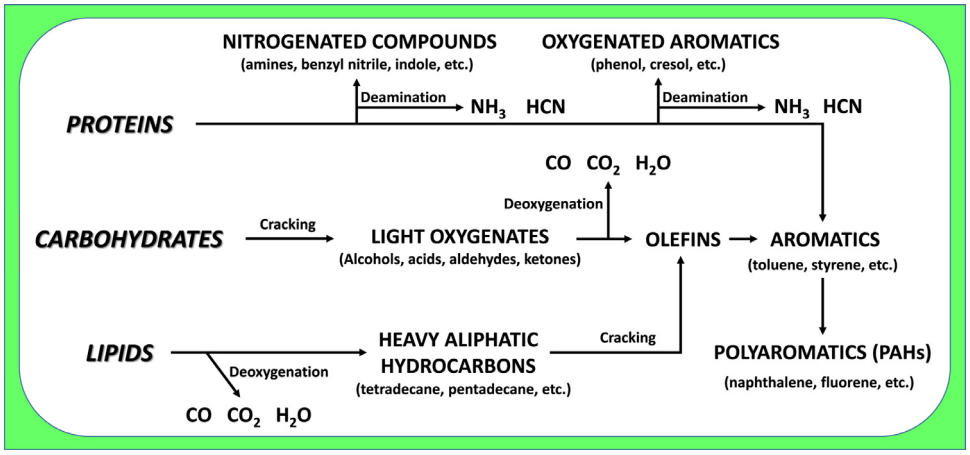


Fig. 6. Proposed scheme showing the main reaction pathways for the microalgae catalytic pyrolysis.

used. This implies that NiCe does not catalyse the addition of N (from proteins deamination) to alkanes and possibly release N as NH_3 is gas phase. Again, the large presence of alkanes in the bio-oil produced using NiCe is supported by the protons abundance in the ^{1}H NMR region between 0 and 1.5 ppm (Table 3).

The catalytic activity of the NiCe/Al_2O_3 and its activity for aromatics production could be explained by the synergies between its metal and acid properties. The Pyridine-FTIR spectra suggest that Lewis and Brønsted acid sites present in the NiCe/Al_2O_3 support and could be linked to the dehydration and subsequent aromatization of the carbohydrate fraction (26% of the starting microalgae) as suggested by the production of benzene substitutes. Previous work showed that strong Brønsted acid sites in HZSM-5 were linked to making large molecules from bagasse to crack into gas molecules, while Lewis acid-selective catalysis resulted in highly efficient bagasse conversion into condensable compounds such as furfural [48].

The pyrolysis of *S. almeriensis* in presence of Ni-based catalysts, resulted in enhanced cracking and reforming of biomass volatiles and tars released.

Overall, all the catalysts tested in this work resulted in large amount of gas yield (44–46 wt%), due to the cracking and reforming effect of combined Ce, Mg and Ni. A similar behaviour was also previously observed for the pyrolysis of a microalgae with a much richer content of protein as *Nannochloropsis* sp. (62%) [26].

4. Conclusions

In this work, the in-situ catalytic pyrolysis of *Pavlova* sp. Microalgae was performed in a fixed-bed reactor in presence of Ce, NiCe and MgCe doped alumina catalysts at different temperatures, being 500 °C the most suitable in terms of bio-oil production. All ceria-based catalysts increased the bio-oil yield with respect to the non-catalytic runs and reduced the O/C ratio from 0.69 (*Pavlova* sp.) to 0.1–0.15, getting closer to that of crude oil. MgCe/Al_2O_3 presented the best performance in terms of bio-oil oxygen concentration, with a reduction of more than 30% of oxygen content with respect to the non-catalytic experiment, from 14.1 to 9.8 wt% O.

Furthermore, from GC–MS analyses is shown that all catalysts favoured decarbonylation and cracking reactions with formation of C_1–C_5 hydrocarbons in gas phase. But also, an increased amount of nitrogen containing compounds (mostly NH_3 and HCN) was released in comparison with the non-catalytic experiment, and in particular in case of MgCe/Al_2O_3.

Overall, these results indicate that NiCe doped alumina could be used to selectively produce hydrocarbons by promoting the deoxygenation and denitrogenation of the *Pavlova* bio-oil sp. to produce aliphatic and aromatic compounds.

Acknowledgments

The authors thank the EPSRC (Grant no. EP/P018955/1) for support and Varicon Aqua Solutions for providing the algae samples. Tevfik Aysu thanks the financial support provided by the post-doctoral research fellowship programme (2219), Scientific and Technological Research Council of Turkey (TUBITAK).

Supplementary materials

Supplementary material associated with this article can be found, in the online version, at doi:10.1016/j.jechem.2017.06.014.

References

[1] K.W. Chew, J.Y. Yap, P.L. Show, N.H. Suan, J.C. Juan, T.C. Ling, D.-J. Lee, J.-S. Chang, Bioresour. Technol. 229 (2017) 53–62.
[2] D.K.Y. Lim, S. Garg, M. Timmins, E.S.B. Zhang, S.R. Thomas-Hall, H. Schuhmann, Y. Li, P.M. Schenk, PLoS One 7 (2012) 1–13.
[3] F. Ahmed, W. Zhou, P.M. Schenk, Algal Res. 10 (2015) 210–217.
[4] M. Hannon, J. Gimpel, M. Tran, B. Rasala, S. Mayfield, Biofuels 1 (2010) 763–784.
[5] K.K. Sharma, H. Schuhmann, P.M. Schenk, Energies 5 (2012) 1532–1553.
[6] M. Stöcker, Angew. Chem. Int. Ed. 47 (2008) 9200–9211.
[7] C. Liu, H. Wang, A.M. Karim, J. Sun, Y. Wang, Chem. Soc. Rev. 43 (2014) 7594–7623.
[8] J. Fermoso, P. Pizarro, J.M. Coronado, D.P. Serrano, WIREs Energy Environ. 6 (4) (2017) 1–18.
[9] H. Hernando, J. Fermoso, I. Moreno, J.M. Coronado, D.P. Serrano, P. Pizarro, Biomass Convers. Biorefinery (2017), doi:10.1007/s13399-017-0262-x.
[10] H. Hernando, S. Jiménez-Sánchez, J. Fermoso, P. Pizarro, J.M. Coronado, D.P. Serrano, Catal. Sci. Technol. 6 (2016) 2829–2843.
[11] Y. Zhang, P. Chen, H. Lou, J. Energy Chem. 25 (2016) 427–433.
[12] G.W. Huber, S. Iborra, A. Corma, Chem. Rev. 106 (2006) 4044–4098.
[13] C. Lorenzetti, R. Conti, D. Fabbri, J. Yanik, Fuel 166 (2016) 446–452.
[14] A. Galadima, O. Muraza, Energy Convers. Manag. 105 (2015) 338–354.
[15] Z. Du, X. Ma, Y. Li, P. Chen, Y. Liu, X. Lin, H. Lei, R. Ruan, Bioresour. Technol. 139 (2013) 397–401.
[16] G. Kabir, B.H. Hameed, Renew. Sustain. Energy Rev. 70 (2017) 945–967.
[17] H. Hernando, I. Moreno, J. Fermoso, C. Ochoa-Hernández, P. Pizarro, J.M. Coronado, J. Čejka, D.P. Serrano, Biomass Convers. Biorefinery (2017), doi:10.1007/s13399-017-0266-6.
[18] C. Mukarakate, M.J. Watson, J. ten Dam, X. Baucherel, S. Budhi, M.M. Yung, H. Ben, K. Iisa, R.M. Baldwin, M.R. Nimlos, Green Chem. 16 (2014) 4891–4905.
[19] H. Cerqueira, P. Ayrault, J. Datka, M. Guisnet, Micropor. Mesopor. Mater. 38 (2000) 197–205.
[20] A. Aho, N. Kumar, K. Eränen, T. Salmi, M. Hupa, D.Y. Murzin, Fuel 87 (2008) 2493–2501.
[21] D.J. Mihalcik, C.A. Mullen, A.A. Boateng, J. Anal. Appl. Pyrolysis 92 (2011) 224–232.

Downloaded to IP: 10.159.164.174 On: 2020-04-23 08:28:51 http://engine.scichina.com/doi/10.1016/j.jechem.2017.06.014

[22] J. Fermoso, H. Hernando, P. Jana, I. Moreno, J. Prech, C. Ochoa-hernández, P. Pizarro, J.M. Coronado, J. Cejka, D.P. Serrano, Catal. Today 277 (2016) 171–181.
[23] O.D. Mante, J.A. Rodriguez, S.D. Senanayake, S.P. Babu, Green Chem. 17 (2015) 2362–2368.
[24] T. Aysu, M.M. Maroto-Valer, A. Sanna, Bioresour. Technol. 208 (2016) 140–148.
[25] T. Aysu, N.A. Abd Rahman, A. Sanna, Energy 103 (2016) 205–214.
[26] T. Aysu, A. Sanna, Bioresour. Technol. 194 (2015) 108–116.
[27] R. Shakya, J. Whelen, S. Adhikari, R. Mahadevan, S. Neupane, Algal Res. 12 (2015) 80–90.
[28] X. Ying, W. Tiejun, M. Longlong, C. Guanyi, Energy Convers. Manag. 55 (2012) 172–177.
[29] S.A. Channiwala, P.P. Parikh, Fuel 81 (2002) 1051–1063.
[30] S.S. Kim, H.V. Ly, J. Kim, E.Y. Lee, H.C. Woo, Chem. Eng. J. 263 (2015) 194–199.
[31] T.M. Brown, P. Duan, P.E. Savage, Energy Fuels 24 (2010) 3639–3646.
[32] D. López-González, M. Fernandez-Lopez, J.L. Valverde, L. Sanchez-Silva, Energy 73 (2014) 33–43.
[33] P. Biller, A.B. Ross, Bioresour. Technol. 102 (2011) 215–225.
[34] W.-H. Chen, B.-J. Lin, M.-Y. Huang, J.-S. Chang, Bioresour. Technol. 184 (2015) 314–327.
[35] I.V. Babich, M. van der Hulst, L. Lefferts, J.A. Moulijn, P. O'Connor, K. Seshan, Biomass Bioenergy 35 (2011) 3199–3207.
[36] A. Campanella, M.P. Harold, Biomass Bioenergy 46 (2012) 218–232.
[37] H. Qiao, Z. Wei, H. Yang, L. Zhu, X. Yan, J. Nanomater. 2009 (2009) 1–5.
[38] J.M. Hernández-Enríquez, R. Silva-Rodrigo, R. García-Alamilla, L. Arcelia García-Serrano, B.E. Handy, G. Cárdenas-Galindo, A. Cueto-Hernández, Chem. Soc 56 (2012) 115–120.
[39] W. Dong, Z. Shen, B. Peng, M. Gu, X. Zhou, B. Xiang, Y. Zhang, Sci. Rep. 6 (2016) 26713.
[40] J. Fermoso, J.M. Coronado, D.P. Serrano, P. Pizarro, Microalgae-Based Biofuels and Bioproducts: From Feedstock Cultivation to End-products, Elsevier Ltd., 2017, pp. 259–282.
[41] F.C. Borges, Q. Xie, M. Min, L.A.R. Muniz, M. Farenzena, J.O. Trierweiler, P. Chen, R. Ruan, Bioresour. Technol. 166 (2014) 518–526.
[42] J. Joyce, Conditioning Biochars for Application to Soils, Technical Note, 2010 http://www.terra-char.com/uploads/2/3/7/9/23790961/composting_with_biochar.pdf.
[43] Y. Yang, J.G. Brammer, A.S.N. Mahmood, A. Hornung, Bioresour. Technol. 169 (2014) 794–799.
[44] K. Wang, Pyrolysis and Catalytic Pyrolysis of Protein- and Lipid-Rich Feedstock, Iowa State University Ames, 2014.
[45] G. Kumar, S. Shobana, W.-H. Chen, Q.-V. Bach, S.-H. Kim, A.E. Atabani, J.-S. Chang, Green Chem. 19 (2017) 44–67.
[46] P.A. Horne, P.T. Williams, Fuel 75 (1996) 1051–1059.
[47] Z. Du, Thermochemical Conversion of Microalgae for Biofuel Production, University of Minnesota, 2013.
[48] S. Leng, X. Wang, Q. Cai, F. Ma, Y. Liu, J. Wang, Bioresour. Technol. 149 (2013) 341–345.

Downloaded to IP: 10.159.164.174 On: 2020-04-23 08:28:51 http://engine.scichina.com/doi/10.1016/j.jechem.2017.06.014